



ARTICLE

# Identification of a novel 4.6-kb genomic deletion in presenilin-1 gene which results in exclusion of exon 9 in a Finnish early onset Alzheimer's disease family: an *Alu* core sequence-stimulated recombination?

Mikko Hiltunen<sup>1,2</sup>, Seppo Helisalmi<sup>1,2</sup>, Arto Mannermaa<sup>2</sup>, Irina Alafuzoff<sup>1,3</sup>, Anne Maria Koivisto<sup>1</sup>, Maarit Lehtovirta<sup>1</sup>, Mia Pirskanen<sup>1,2</sup>, Raimo Sulkava<sup>4</sup>, Auli Verkkoniemi<sup>5</sup> and Hilikka Soininen<sup>1</sup>

<sup>1</sup>Department of Neurology, University Hospital and University of Kuopio; <sup>2</sup>Chromosome and DNA Laboratory of the Division of Diagnostic Services; <sup>3</sup>Department of Pathology, University Hospital of Kuopio; <sup>4</sup>Department of Public Health and General Practice, Division of Geriatrics, University and University Hospital of Kuopio; <sup>5</sup>Department of Clinical Neuroscience, Helsinki University Central Hospital, Finland

Mutations in the presenilin-1 (*PS-1*) gene have been shown to cause early onset Alzheimer's disease (EOAD) in an autosomal dominant manner. We have identified a novel 4.6-kb genomic deletion in the *PS-1* gene in a Finnish EOAD family, which leads to an inframe exclusion of exon 9 ( $\Delta 9$ ) from the mRNA transcript. This germline mutation results in a similar alteration in mRNA level as previously described with the variant AD and the  $\Delta 9$  splice-site mutations. In this present EOAD family, the clinical and neuropathological phenotype of patients are those of the typical AD without indications of spastic paraparesis or 'cotton wool' plaques, which are the hallmarks of the variant AD. A sequence analysis of the deletion crossover site of the mutant and corresponding wild type regions revealed complete homology with the recombinogenic 26 bp *Alu* core sequence at intron 8. In addition, a segment at the intron 9 breakpoint displayed homology with the core sequence, but comparison of the 5' and 3' breakpoint sequences did not reveal significant identity favouring involvement of *Alu* core sequence-stimulated non-homologous recombination rather than *Alu*-mediated homologous pairing of the fragments. This study shows that large genomic rearrangements can affect the EOAD gene *PS-1* through a mechanism, which may involve *Alu* core sequence-stimulated recombination. *European Journal of Human Genetics* (2000) 8, 259–266.

**Keywords:** Alzheimer's disease; presenilin-1; genomic deletion; *Alu* core sequence; non-homologous recombination; substitution E318G

## Introduction

Alzheimer's disease (AD) is the most common cause of progressive neurological disorder leading to dementia. It is neuropathologically characterised by senile plaques and

neurofibrillary tangles in the cortex of the brain. The molecular mechanisms leading to AD are not well understood, but it has a genetic etiology, which is most evident in the case of early onset AD (EOAD). To date, highly penetrant mutations in three genes are known to cause autosomal dominant EOAD (onset age before 65 years): amyloid precursor protein (*APP*) gene on chromosome 21, presenilin-1 (*PS-1*) gene on chromosome 14 and presenilin-2 (*PS-2*) gene on chromosome 1.<sup>1–4</sup> Together, these genes account for approximately 1% of the total AD population while the

Correspondence: Mikko Hiltunen, MSc, Chromosome and DNA Laboratory, Kuopio University Hospital, P.O. Box 1777, FIN-70211 Kuopio, Finland. Tel: +358 17 172729; Fax: +358 17 172726; E-mail: mhiltune@messi.uku.fi  
Received 31 August 1999; revised 7 October 1999; accepted 8 November 1999

mutations within the *PS-1* gene are more frequently by the cause of EOAD than the mutations in other known genes.

Over 50 different *PS-1* gene mutations have been reported in approximately 80 families of various ethnic origins. Nearly all the molecular genetic changes are missense mutations leading to increased production of amyloidogenic A $\beta$ 42 peptide by gain-of-function or dominant-negative mechanism affecting the APP processing. The exceptions are the splice-site mutations resulting in an inframe skipping of exon 9 ( $\Delta$ 9) accompanied by a point mutation at the splice junction codon 290 (S290C), and the deletion of exon 9 from the mRNA by an yet undetermined mechanism.<sup>5-8</sup> In addition, mutation in the intron 4 splice site junction of the *PS-1* gene results in two shortened transcripts with premature termination codons and one full-length transcript with insertion of three nucleotides.<sup>9,10</sup> However, *in vivo* experiments showed only the presence of the full-length PS-1 protein with one extra amino acid (Thr) in brain extracts and lymphoblast lysates of mutation carriers. PS-1  $\Delta$ 9 mutations lead to the exclusion of 28 amino acids from the cytoplasmic loop domain of the protein, which contains the endoproteolytic cleavage site. In the normal physiological situation, PS-1 holoprotein undergoes well-controlled proteolytic processing, which produces about 17 kDa carboxyl-terminal and about 28 kDa amino-terminal fragments. Lack of the cleavage

site in  $\Delta$ 9 deletions results in the accumulation of uncleaved PS-1 protein. Recently, it was shown that the point mutation (S290C) at the exon 8/10 splice junction rather than the lack of proteolytic processing of *PS-1* in the  $\Delta$ 9 mutation, is the cause of the enhancement of pathological functions.<sup>11</sup>

In this study, we have identified a novel 4.6-kb genomic deletion in the *PS-1* gene leading to exclusion of exon 9 in a Finnish EOAD family. AD patients carrying this genomic deletion showed the typical phenotypic features of AD without indications of spastic paraparesis or 'cotton wool' plaques described in the variant AD patients.<sup>8</sup> We suggest here that the *Alu* core sequence-stimulated non-homologous event may underlie the genomic rearrangement in this particular EOAD family.

## Family and methods

### Family

The family had several members with early onset dementia and the transmission of the disease indicated autosomal dominant inheritance (Figure 1). We were able to perform neurological examinations, neuropsychological tests, CT scanning and differential diagnostic laboratory tests for three affected individuals (II:2, II:4 and II:5). For patient II:2, EEG, SPECT, and psychiatric evaluation were made and the patient was diagnosed as having probable AD. Brain biopsy was taken

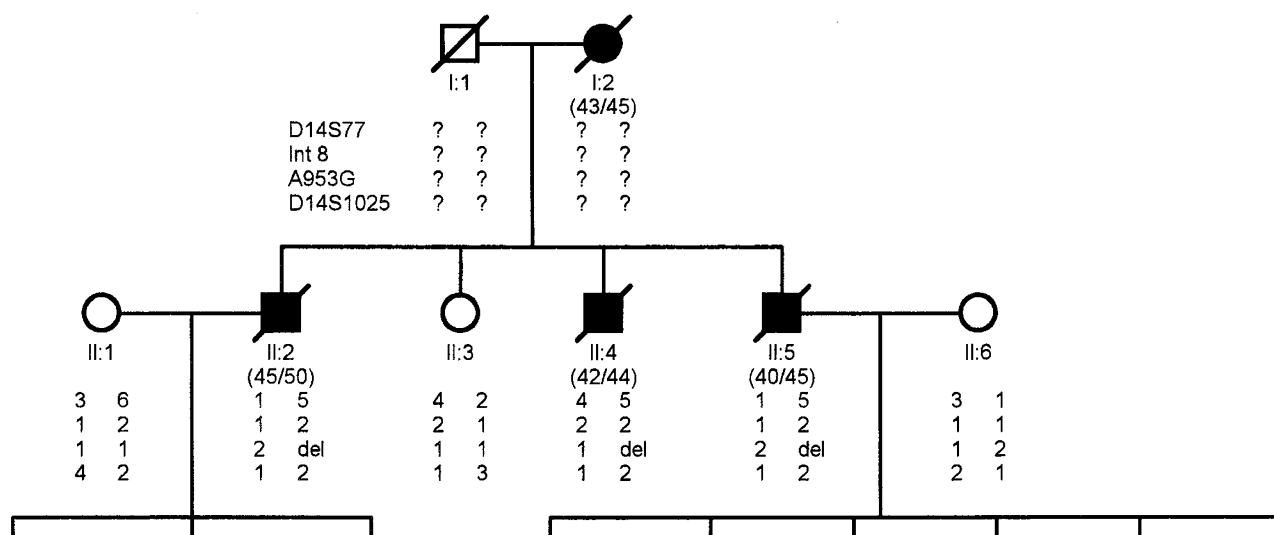


**Figure 1** Haplotype analysis with markers flanking or within the *PS-1* gene on chromosome 14. Affected individuals are denoted by a filled symbol and the ages at onset and at death, respectively, are indicated in parentheses. Haplotype 5-2-del-2 is shared by affected family members (II:2 = probable AD; II:4 = definite AD; II:5 = probable AD). Int 8 = intron 8 polymorphism; A953G = A (1) to G (2), a substitution leading to the amino acid change from glutamic acid to glycine at the codon 318 (E318G).

from patient II:4 and the definite AD was diagnosed (see neuropathology). Patients II:2, II:4 and II:5 were regularly examined by neurologists after the disease onset. Patient I:2, who had died long before our present study, was clinically examined in the 1970s and was diagnosed as demented. In addition, 51 control subjects and 102 familial and sporadic early and late onset AD patients from Eastern Finland, who fulfilled the NINCDS-ADRDA criteria for definite, probable, or possible AD<sup>12</sup> were used for mutation screening.

#### DNA extraction

Genomic DNA was extracted from white blood cells by a standard procedure<sup>13</sup> and from paraffin-embedded tissues in postmortem AD cases as described by Isola *et al*<sup>14</sup>

#### Sequence analysis

The exons of open reading-frame of the *PS-1* gene (exons 3–12) were PCR amplified with similar primers and conditions as reported by Hutton *et al*.<sup>15</sup> PCR products were purified and cycle-sequenced with the ABI PRISM310 genetic analyser (Perkin Elmer, Foster City, CA, USA) by utilising the dReady Dye Terminator Cycle Sequencing kit with AmpliTaq DNA polymerase, FS (Perkin Elmer, Foster City, CA, USA).

#### Haplotyping

Microsatellite markers D14S77 and D14S1025 were genotyped using fluorescent-labelled PCR-primers obtained from the Genome Database (<http://gdbWWW.gdb.org/>). PCR amplifications were performed using the standard procedure.<sup>16</sup> The sizes of PCR products were determined with ABI PRISM 310 genetic analyser (Perkin Elmer). Intron 8 polymorphism and E318G substitution in exon 9 were analysed by PCR using mismatch primers and restriction enzyme analysis as previously described by Wragg *et al*<sup>17</sup> and Dermaut *et al*,<sup>18</sup> respectively.

#### RT-PCR analysis

Total RNA was extracted from peripheral lymphocytes using Trizol Reagent (Gibco BRL, Grand Island, NY, USA). Poly (A<sup>+</sup>) mRNA was captured using mRNA Capture Kit (Boehringer Mannheim GmbH, Germany) followed by RT-PCR (Titan™ One Tube RT-PCR System, Boehringer Mannheim) with exons 8 (DEL9F: 5'-GCT GTT TTG TGT CCG AAA GGT CCA CTT CGT ATG CTG-3') and 10 (DEL9R: 5'-CTC TGG GTC TTC ACC AGC GAG GAT ACT GCT GGA AAG-3') specific primers (Figure 3B). Truncated 261 bp PCR product was excised from 1% low melting agarose gel and cycle-sequenced in both directions (see sequence analysis of PS-1 exons).

#### Genomic DNA analysis

To define the deletion breakpoint region, PCR reactions were carried out using different primer pairs located at the introns 8 and 9 with Expanded Long PCR System (Boehringer Mannheim). A reaction with primers IN8F4 (5'-AAG TGG TTC ACT CTG GGA GCT TAA C-3') and IN9F5 (5'-GAA AGC

TCT TCC TCC ATC CTT CAG C-3') (Figure 3B) revealed a novel 1.6-kb PCR-product, which was seen only in the affected member of the family. The PCR-product was cycle-sequenced in both directions. For diagnostic purposes, multiplex PCR primers DE8F1 (5'-GTG GAC ATT GAT TTT CAT GTT AC-3'), DE8R2 (5'-TCT AAT ACT CAG GCT TCT TGA AG-3') and DE9R1 (5'-TAT ACC TAC ATG CTC ACA GAC AAT C-3') (Figure 3B) were designed on the basis of sequence data to amplify control (504 bp) and deleted (290 bp) fragments. The cycle parameters were 3 min initial denaturation at 94°C followed by 30 cycles at 94°C for 1 min, 52°C for 45 s, and 72°C for 1 min. *Alu* and other repeat sequences were identified using the BLAST 2.0 program (<http://www.ncbi.nlm.nih.gov/>) and the Repeat Masker Server (<http://ftp.genome.washington.edu/>).

#### Neuropathology

Cortical biopsy taken in 1992 from the patient II:4 was in two pieces, each approximately 10 mm in diameter. After fixation and paraffin embedding seven-µm thick sections were cut and stained with hematoxylin-eosin, thioflavin-S and modified Bielschowsky silver impregnation. Furthermore, with immunohistochemical stainings, β-amyloid aggregates (βA4 – DAKO (Glostrup, Denmark) M872, dilution 1:100; βA40 and βA42 – US Peptides (New York, NY, USA) 1:1500; 4G8 and 6E10 – Senetek (St. Louis, MO, USA) 1:2000), neurofibrillary tangles (AT8 – Innogenetics (Ghent, Belgium) BR03, 1:500), Lewy inclusions and threads (Synuclein 1, Transduction Lab (Los Angeles, CA, USA) S63320, 1:1000; α-synuclein, ZYMED (San Francisco, CA, USA) LB509, 1:500), reactive astrocytes (GFAP – DAKO Z0334) and activated microglia (HLA DR – DAKO M775) and complement components (C1q – DAKO A0136, C3c – DAKO A0062, C3d – DAKO A0063 and C5 – DAKO A0055, 1:100) were visualised.

#### Results

A substitution E318G in exon 9, which was recently shown not to relate causally to AD,<sup>18</sup> was detected in two affected cases and in eight healthy individuals by sequencing the coding region of *PS-1* (Figure 1). No other *PS-1* gene alterations were detected. Five out of ten substitution carriers were homozygous for the E318G variant. Segregation of the E318G substitution from the family members to their offspring did not follow normal Mendelian inheritance patterns, since genetic inconsistency was observed in some individuals. To determine the cause of this inconsistency, two microsatellite markers around the *PS-1* gene and one biallelic marker located at the 5' end of intron 8 were analysed to construct extended haplotypes. All markers showed a normal segregation pattern. Therefore, the most likely explanation for the non-Mendelian segregation pattern of the E318G substitution was a heterozygous deletion around exon 9, which was defined to start downstream from the biallelic marker of intron 8. Upon further scrutiny, all the AD cases carried the same haplotype 5-2-del-2 for D14S77, intronic polymor-

phism, E318G, and D14S1025, respectively.

RT-PCR analysis using a lymphocyte sample carrying the presumed disease-associated haplotype 5-2-del-2 was performed (Figure 2A). A truncated 261 bp fragment was revealed with PCR-primers located within the exons 8 and 10 (Figure 3B), and the sequence analysis of the abnormal RT-PCR fragment showed an inframe deletion of codons 290–319 corresponding to exon 9 (data not shown). In accordance with this result, RT-PCR performed with exon 7 and 12 specific primers produced a truncated fragment lacking the alternatively spliced exon 8<sup>19</sup> and also exon 9 (data not shown). Therefore, abnormal exclusion of the exon 9 from PS-1 cDNA suggested that the breakpoint regions of genomic deletion were located in the introns 8 and 9.

In order to define the deletion breakpoints at the genomic level, long PCR amplifications with intron 8 and 9 specific primers were conducted. A PCR reaction with primers IN8F4 and IN9F5 located approximately 2.7 and 3.3-kb from exon 9, respectively (Figure 3B), produced a novel 1.6-kb fragment, which was only seen in the affected family member (data not shown). Diagnostic PCR primers were designed on the basis of sequence data obtained from 1.6-kb product (Figure 3B) and the screening of the affected family members showed a heterozygote 290 bp fragment in subjects carrying the haplotype 5-2-del-2 (Figure 2B). Sequence analysis of the 290 bp fragment revealed flanking sequences of the deletion. This

allowed us to determine that the total deletion was 4555 bp large and consists of 1.6-kb distal part of intron 8, exon 9 and a 2.9-kb proximal part of intron 9 (Figures 3A and B). Deletion analysis of 102 AD patients and 51 control subjects from Eastern Finland did not reveal any additional cases with the novel PS-1  $\Delta$ 9 mutation.

In the neuropathological examination, the Hematoxylin-Eosin staining of the frontal cortex sections visualised both grey and white matter. In the grey matter characteristic lesions for AD, such as amyloid plaques (AP) with a central core formation and neurofibrillary tangles among the neuronal population were observed (Figure 4A). Round plaques without cellular participation as described in the entity of variant AD with cotton wool plaques were not seen. Thioflavin-S staining demonstrated several amyloid cores and cerebral amyloid angiopathy (CAA), both in the parenchyme and in the leptomeninges. Bielshowsky silver impregnation demonstrated numerous neurofibrillary tangles, neuritic plaques and senile/amyloid plaques (Figure 4B). Alzheimer's degenerative changes were sufficient for the diagnosis of definite AD according to CERAD.<sup>20</sup> Beta-amyloid aggregates were visualized with immunohistochemical staining (Figure 4C) in the vessel walls of the neuropil and leptomeninges (CAA) and in the neurophil as APs. These APs were quite numerous, round in shape and varied in size. Numerous APs and CAA were labelled with antibodies  $\beta$ A4,  $\beta$ A42, 6E10 and

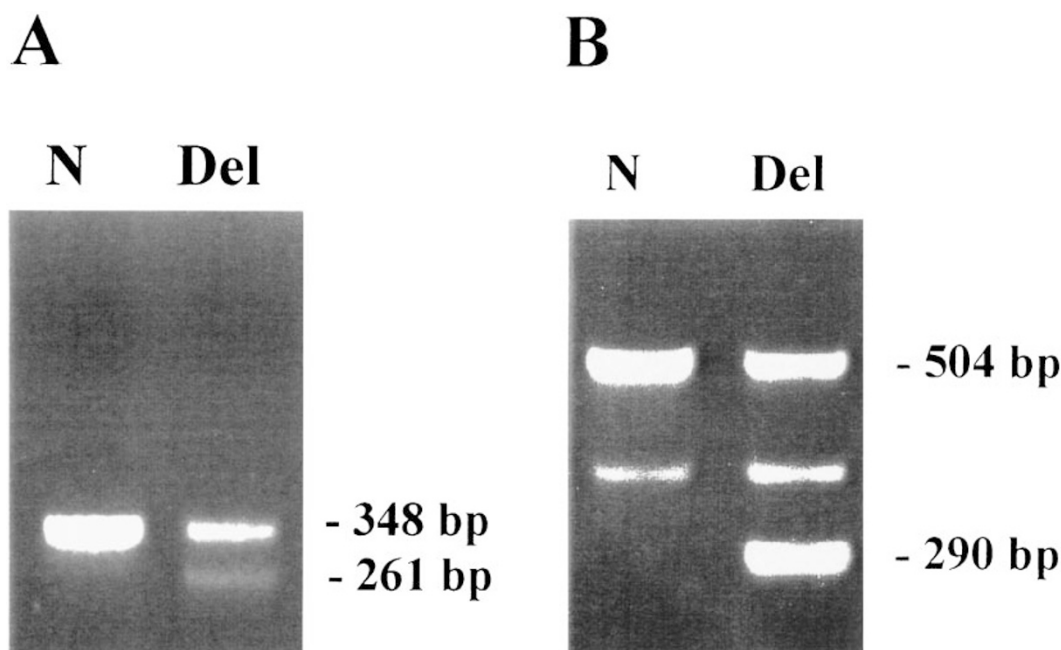


**Figure 2** Molecular analysis of the PS1 deletion. N = normal; Del = deletion. **A** RT-PCR analysis of RNA extracted from lymphocytes. To avoid alternatively spliced fragments of exon 8 produced in lymphocytes, cDNAs were amplified using exon 8 and 10 specific primers. Truncated 261 bp fragment including the exons 8 and 10 was excised from the agarose gel and sequenced. **B** DNA analysis of genomic deletion using the intron 8 and 9 specific PCR-primers. Multiplex PCR reactions with primers DE8F1, DE8R2 and DE9R1 were performed to amplify control (504 bp) and deleted fragments (290 bp). The intermediate DNA fragment seen in both AD and control cases was the product of unspecific PCR-amplification.

4G8 whereas only few were labelled with antibodies against the short  $\beta$ A40. Some amyloid aggregates were also detected in the white matter. Numerous neurofibrillary tangles (NFT), neuropil threads (NT) and neurites in neuritic plaques (NP) were visualised with phosphorylated PHF-Tau antibody (Figure 4D). Furthermore, positive NTs were also seen in the

white matter. Intra neuronal inclusions labelled with synuclein-1 or with  $\alpha$ -synuclein antibodies could not be detected, even though the latter antibody labelled some of the plaques. Prion protein staining did not reveal changes seen in prion diseases. Quite strong inflammatory response was noted both as numerous activated microglial cells (AM) and reactive

## A

Intron 8	GCATAAAGAA	AGAAAACCTA	ATAAATCGCT	GGTGGCTTCA	TTTCCAAAAG
Deletion	GCATAAAGAA	AGAAAACCTA	ATAAATCGCT	GGTGGCTTCA	TTTCCAAAAG
Intron 9	CAGCTCACAG	AGCATGCTGC	CCCAGCTGCA	CCTCCCCTGC	TGCAGCTGCC
Intron 8	GCTATGGAAA	TCCATAAACA	<u>GGCtgggTGC</u>	<u>AGTGGCTCAT</u>	<u>GCCTGTAATC</u>
Deletion	GCTATGGAAA	TCCATAAACA	GGCtgggCCG	CTGCTGCCAT	CAAGACCACT
Intron 9	<u>ATCTTTGCAG</u>	<u>CAGCCACTCC</u>	AGAtgggCCG	CTGCTGCCAT	CAAGACCACT
Intron 8	<u>CTAGCACTTT</u>	<u>GGGAGGCTGA</u>	<u>GGCGGGAGGA</u>	<u>TTGCTTGAGC</u>	<u>CCAGGAGTTT</u>
Deletion	AGTAAACCTG	ATAGAAAAGT	AAGAAATATA	CTGGAAAGAA	TTGCCACAAG
Intron 9	AGTAAACCTG	ATAGAAAAGT	AAGAAATATA	CTGGAAAGAA	TTGCCACAAG
Intron 8	GAGTCTGGCC	TGGGCAACGT	AGTGAGACCC	TGTTTTTAGA	AAAAATGAAG
Deletion	CCTGGCTCTT	GTGTTAACCT	GTGTTAAGCT	AAAGAAAATC	AAATGATTGT
Intron 9	CCTGGCTCTT	GTGTTAACCT	GTGTTAAGCT	AAAGAAAATC	AAATGATTGT
Intron 8	<u>ATAAAAAACT</u>	<u>AATCCATAAA</u>	<u>CCTCATACTT</u>	<u>GGTGGTTGCC</u>	<u>CTTCAGTTTT</u>
Deletion	CTGTGAGCAT	GTAGGTATAT	ATGTATGTGA	GTGAGTGATA	CAACAGAATT
Intron 9	CTGTGAGCAT	GTAGGTATAT	ATGTATGTGA	GTGAGTGATA	CAACAGAATT

## B

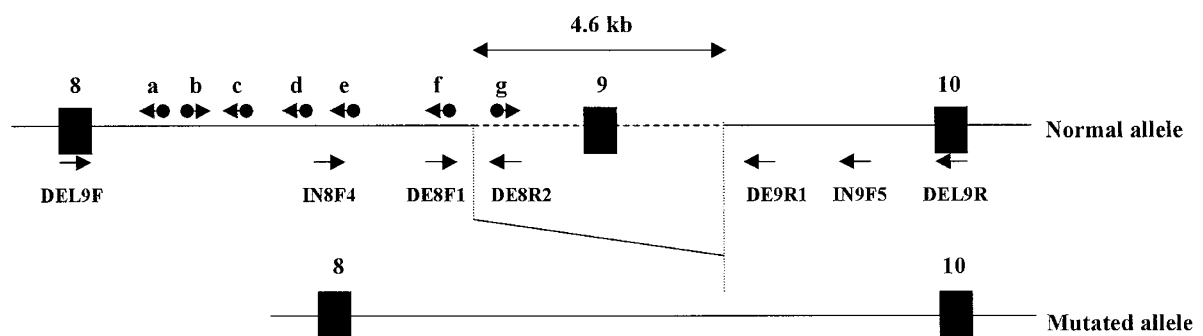


**Figure 3** Sequence analysis of the region flanking the deletion crossover site. **A** Genomic sequences of *PS-1* involved in the recombination process. Recombinogenic 26 bp *Alu* core sequence (double line) and a sequence displaying homology with FLAM C repeat sequence (underlined) located in the intron 8 are shown. The presumed homology segment for *Alu* core sequence is indicated in the intron 9 (dashed line). **B** Schematic presentation of the normal and mutated alleles of *PS-1* gene. The location and orientation of PCR primers (arrows) and human *Alu* consensus sequences (modified arrows) are indicated in the introns 8 and 9. *Alu* subfamily sequences are composed of two homologous portions arranged in a head to tail dimer of approximately 130 bp.

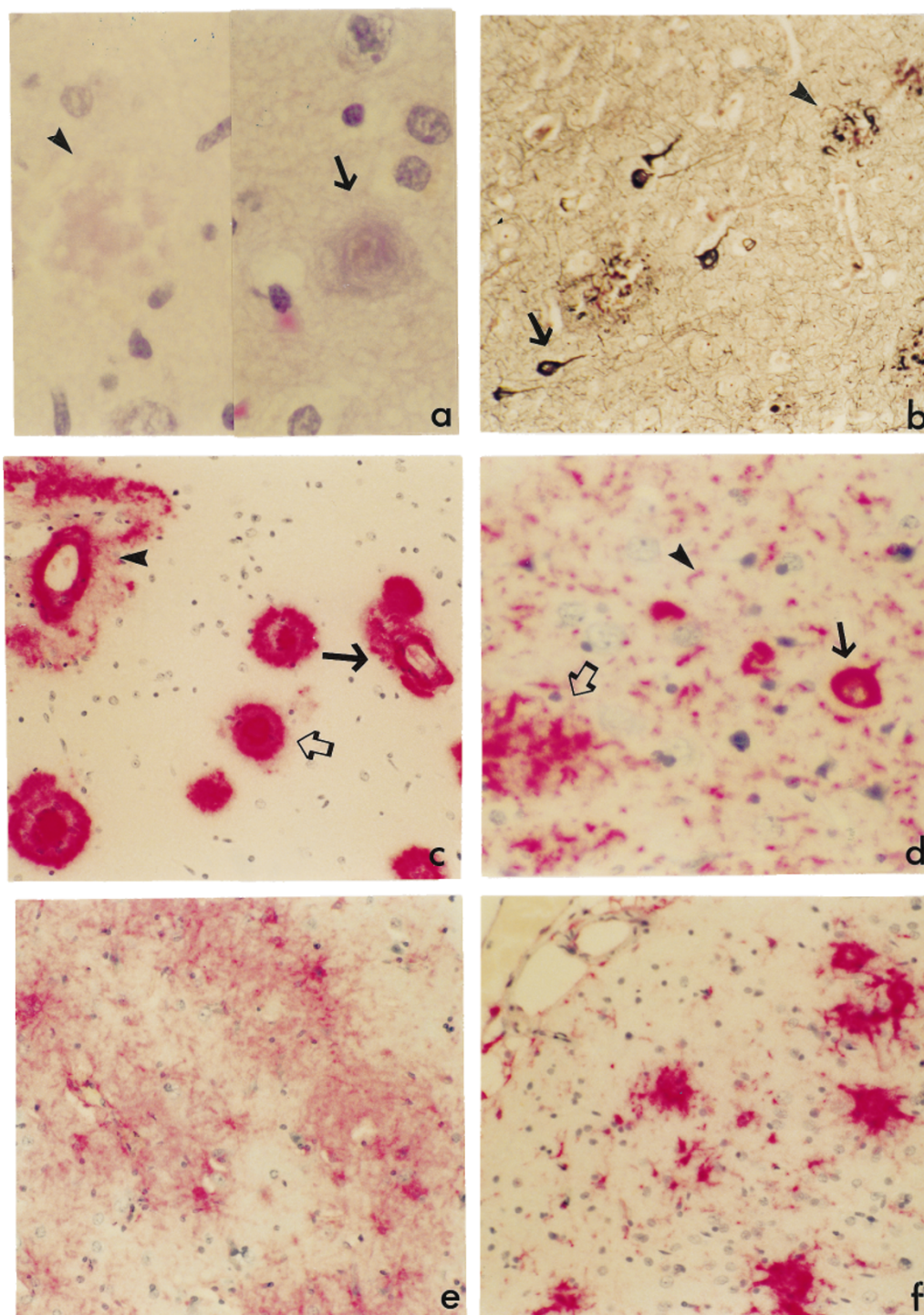


**Figure 4** Neuropathological examination of the frontal cortex section. **A** Hematoxylin-eosin staining, magnification  $200\times$ . Note amyloid plaques (AP) with central core formation. **B** Bielschowsky silver impregnation, magnification  $100\times$ . Note numerous NFTs (arrow) and neuritic plaques (arrowhead). **C** Immunohistochemical labelling of  $\beta$ A4 protein, magnification  $100\times$ . Labelling is seen in the neuropil (open arrow) as APs and in the vessel walls as CAA, of both the neuropil (arrow) and the leptomeninges (arrowhead). **D** Immunohistochemical labelling of neurofibrillary degeneration (AT8), magnification  $200\times$ . Numerous NFTs (arrow), neuropil threads (NT) (arrowhead) and neurites in neuritic plaques (NP) (open arrow) can be seen. **E** Immunohistochemical labelling of reactive astrocytes (GFAP), magnification  $100\times$ . Note numerous reactive astrocytes diffusely within the grey matter. **F** Immunohistochemical labelling of activated microglia (HLA DR), magnification  $100\times$ . Note numerous activated microglial cells primarily located centrally in the plaques.



astrocytes (RA). AMs (Figure 4F) were primarily located centrally in the plaques, whereas the RAs (Figure 4E) were seen more diffusely within the grey matter. Both cell types were also identified within the white matter. Moderate complement factor labelling was observed in association with the plaques with antibodies directed to the C3d factor, and weak staining with antibodies directed to C3c and C1q factors, also in association with the plaques, whereas no staining was detected with antibodies directed to the C5 complement factor.

## Discussion

Recently, Crook *et al*<sup>6</sup> described a novel variant form of AD in a Finnish pedigree with spastic paraparesis and unusual eosinophilic plaques resembling cotton wool balls. These plaques showed uneven peripheral immunoreactivity for A $\beta$  and were not discernible from the background by Thioflavin-S. The molecular genetic basis of the variant form of AD was shown to be a deletion of exon 9 from the PS-1 mRNA, whereas no genomic DNA alteration was identified. In this present article, we have identified a novel 4.6-kb genomic deletion in the *PS-1* gene in one Finnish EOAD family, which leads to the inframe exclusion of exon 9 from the mRNA transcript. Although the genomic deletion leads to a similar end result at the mRNA level as described by Crook *et al*,<sup>6</sup> the phenotypic features of the AD patients clearly resemble the typical AD rather than the variant AD.

Disease-causing genomic rearrangements including large deletions, inversions or duplications, have not been previously demonstrated to occur in the *EOAD* genes. In contrast, germline and somatic rearrangements of the genomic DNA are frequent in various cancer types, and a common mechanism giving rise to these alterations is *Alu*-mediated homologous recombination.<sup>21,22</sup> The well-conserved region of *Alu* sequences is frequently found at or close to the sites of homologous and non-homologous recombination and has been proposed to be a hot spot of recombination.<sup>23</sup> Also in this particular case, a complete 26 bp *Alu* core sequence was located near the tetranucleotide sequence TGGG shared by the both recombining fragments at the intron 8 (Figure 3A). In addition, a small segment upstream from the TGGG sequence displayed homology with the core sequence also in the 3' breakpoint region, indicating involvement of the *Alu* core element, or part of it, in both recombining fragments. Comparison of the breakpoint regions and the nearby intron regions, however, did not reveal any major homology between 5' and 3' sequences favoring the *Alu* core sequence-stimulated non-homologous recombination rather than the *Alu*-mediated homologous pairing of the fragments. Thus, in accordance with findings showing the involvement of at least one complete or partial *Alu* core element in the rearrangement processes,<sup>24,25</sup> the present study also addresses the importance of *Alu* core sequence-stimulated functions in the non-homologous recombination events.

The clinical history of AD patients with the novel *PS-1*  $\Delta 9$  mutation did not reveal any indications of spastic paraparesis (paralysis of legs) or any other major motor-neuronal disturbances. This is crucial since spastic paraparesis is the main clinical feature associated with variant AD patients.<sup>6</sup> In contrast, the common clinical manifestations in AD patients described here are memory impairment and rapid progression of the disease after onset. The mean disease onset age in this EOAD family is 43.5 years, which is close to that previously reported with the  $\Delta 9$  splice-site mutation family.<sup>5</sup> Very early onset ages (from 40 to 45 years of age) with the novel  $\Delta 9$  mutation, is in agreement with the findings showing that the deletion of the PS-1 exon 9 has the greatest impact on A $\beta$ 42 production in various transfected cell lines<sup>26,27</sup> and this is suggested to promote cerebral A $\beta$  deposition and induce AD.<sup>28</sup> In accordance with the clinical features, neuropathology was typical of AD in this family with numerous amyloid plaques with a central core formation, neurofibrillary tangles, neuritic plaques, and reactive astrocytes and microglial cells in association with the plaques. More importantly, neuropathological examination did not reveal 'cotton wool' plaques, which are the hallmark of the variant AD. The phenotypic data, therefore, suggests a clear difference between the variant AD patients with spastic paraparesis and the EOAD patients described here, although the molecular genetic basis in both cases is the abnormal splicing of exon 9.

In addition to the large genomic deletion found in the *PS-1* gene, a substitution E318G was detected in the exon 9 among the family members. The role of the E318G variant is controversial, since it has been reported to be causative for AD,<sup>29</sup> but also to be a rare polymorphism not associated with AD.<sup>18</sup> Our studies using the Finnish AD and control population indicate that the E318G variant is probably non-pathogenic since a small group of age-matched control subjects also carries the alteration (S Helisalmi *et al*, 1999, unpublished data). However, the allele frequency of the E318G variant is significantly increased in both familial and sporadic AD groups when compared with the control group, suggesting that it may be a risk factor in AD. It is possible that the variant is in linkage disequilibrium with yet another change located perhaps in the promoter or regulatory regions of the *PS-1* gene. The effect of the E318G variant on this particular family could be evaluated by a suggestion made by Mehta *et al*.<sup>27</sup> The age of onset of the PS-1-caused disease could be influenced by other genetic factors contributing either in a *cis*- or *trans*-acting way. In this respect, however, the E318G variant does not seem to modulate the age of onset in this family (Figure 1) and its possible role in AD remains to be determined in further studies.

In conclusion, we have identified a novel 4.6-kb genomic deletion in the *PS-1* gene in a Finnish EOAD family, which leads to the exclusion of exon 9 from the PS-1 mRNA. We propose that an *Alu* core-stimulated non-homologous recombination event underlies this rearrangement. Moreover, we

could not detect further cases with the mutation, indicating that the frequency of this novel  $\Delta 9$  alteration in the Eastern Finnish AD population is low. The expression of both the wild type and truncated PS-1 transcripts probably rules out the possibility that pathogenic effects would be exerted through haploinsufficiency. Therefore, the possible mechanism of pathogenesis in this novel  $\Delta 9$  mutation may be the same as previously suggested by Citron *et al*<sup>28</sup> and Ishii *et al*.<sup>30</sup> Increased production and deposition of amyloidogenic A $\beta$ 42 could then be the fundamental pathological determinant promoting AD. Finally, the phenotypic differences between various  $\Delta 9$  mutation families suggest that there exist modifying factors, which may participate in the AD process in addition to the main causative agent.

# Acknowledgements

The authors thank Dr Garry Wong for helpful comments and Ms Marjo Heikkinen for skilful technical help. The study was supported by the Health Research Council of the Academy of Finland, EVO grants (5032 and 5142) of Kuopio University Hospital and the Helsingin Sanomat Centennial Foundation. MH and SH contributed equally to this work.

# References

- Goate AM, Chartier-Harlin MC, Mullan M *et al*: Segregation of a missense mutation in the amyloid precursor protein gene with familial Alzheimer's disease. *Nature* 1991; **349**: 704–706.
- Sherrington R, Rogaev EI, Liang Y *et al*: Cloning of a gene bearing missense mutations in early-onset familial Alzheimer's disease. *Nature* 1995; **375**: 754–760.
- Levy-Lahad E, Wasco W, Poorkaj P *et al*: Candidate gene for the chromosome 1 familial Alzheimer's disease locus. *Science* 1995; **269**: 973–977.
- Rogaev EI, Sherrington R, Rogaeva EA *et al*: Familial Alzheimer's disease in kindreds with missense mutations in a gene on chromosome 1 related to the Alzheimer's disease type 3 gene. *Nature* 1995; **376**: 775–778.
- Perez-Tur J, Froelich S, Prihar G *et al*: A mutation in Alzheimer's disease destroying a splice acceptor site in the presenilin-1 gene. *NeuroReport* 1995; **7**: 297–301.
- Kwok JB, Taddei K, Hallupp M *et al*: Two novel (M233T and R278T) presenilin-1 mutations in early-onset Alzheimer's disease pedigrees and preliminary evidence for association of presenilin-1 mutations with a novel phenotype. *NeuroReport* 1997; **8**: 1537–1542.
- Sato S, Kamino K, Miki T *et al*: Splicing mutation of presenilin-1 gene for early-onset familial Alzheimer's disease. *Hum Mutat* 1998; **1**: Suppl. 91–94.
- Crook R, Verkkoniemi A, Perez-Tur J *et al*: A variant of Alzheimer's disease with spastic paraparesis and unusual plaques due to deletion of exon 9 of presenilin 1. *Nat Med* 1998; **4**: 452–455.
- Tysoe C, Whittaker J, Xuereb J *et al*: A presenilin-1 truncating mutation is present in two cases with autopsy-confirmed early-onset Alzheimer's disease. *Am J Hum Genet* 1998; **62**: 70–76.
- De Jonghe C, Cruts M, Rogaeva EA *et al*: Aberrant splicing in the presenilin-1 intron 4 mutation causes presenile Alzheimer's disease by increased A $\beta$ 42 secretion. *Hum Mol Genet* 1999; **8**: 1529–1540.
- Steiner H, Romig H, Crim MG *et al*: The biological and pathological function of the presenilin-1 Delta exon 9 mutation is independent of its defect to undergo proteolytic processing. *J Biol Chem* 1999; **274**: 7615–7618.
- McKhann G, Drachman D, Folstein M, Katzman R, Price D, Stadlan EM: Clinical diagnosis of Alzheimer's disease: report of the NINCDS-ADRDA Work Group under the auspices of Department of Health and Human Services Task Force on Alzheimer's Disease. *Neurology* 1984; **34**: 939–944.
- Vandenplas S, Grobler-Rabie A, Brebner K *et al*: Blot hybridization of genomic DNA. *J Med Genet* 1984; **21**: 164–172.
- Isola J, Devries S, Chu L, Ghazvin S, Waldman F: Analysis of changes in DNA sequence copy number by comparative genomic hybridization in archival paraffin-embedded tumor samples. *Am J Pathol* 1994; **145**: 1301–1308.
- Hutton M, Busfield F, Wragg M *et al*: Complete analysis of the presenilin 1 gene in early onset Alzheimer's disease. *NeuroReport* 1996; **7**: 801–805.
- Sheffield VC, Weber JL, Buetow KH *et al*: A collection of tri- and tetranucleotide repeat markers used to generate high quality, high resolution human genome-wide linkage maps. *Hum Mol Genet* 1995; **4**: 1837–1844.
- Wragg M, Hutton M, Talbot C, the Alzheimer's disease collaborative group: Genetic association between intronic polymorphism in presenilin-1 gene and late-onset Alzheimer's disease. *Lancet* 1996; **347**: 509–512.
- Dermaut B, Cruts M, Slaughter AJC *et al*: The Glu318Gly substitution in presenilin 1 is not causally related to Alzheimer's disease. *Am J Hum Genet* 1999; **64**: 290–292.
- Rogaev EI, Sherrington R, Wu C *et al*: Analysis of the 5' sequence, genomic structure, and alternative splicing of the presenilin-1 gene (*PSEN1*) associated with early onset Alzheimer's disease. *Genomics* 1997; **40**: 415–424.
- Mirra SS, Heyman A, McKeel D *et al*: The Consortium to establish a registry for Alzheimer's disease (CERAD). Part II. Standardization of the neuropathologic assessment of Alzheimer's disease. *Neurology* 1991; **41**: 479–486.
- Nyström-Lahti M, Kristo P, Nicolaides NC *et al*: Founding mutations and *Alu*-mediated recombination in hereditary colon cancer. *Nat Med* 1995; **1**: 1203–1206.
- Puget N, Sinilnikova OM, Stoppa-Lyonnet D *et al*: An *Alu*-mediated 6-kb duplication in the *BRCA1* gene: a new founder mutation. *Am J Hum Genet* 1999; **64**: 300–302.
- Rüdiger NS, Gregersen N, Kielland-Brandt MC: One short well-conserved region of *Alu*-sequence is involved in human gene rearrangements and has homology with prokaryotic *chi*. *Nucleic Acids Res* 1995; **23**: 256–260.
- Henthorn PS, Mager DL, Huisman THJ, Smithies O: A gene deletion ending within a complex array of repeated sequence 3' to the human beta-globin gene cluster. *Proc Natl Acad Sci USA* 1986; **83**: 5194–5198.
- Myerowitz R, Hogikyan ND: A deletion involving *Alu* sequences in the beta-hexosaminidase alpha-chain gene of French Canadians with Tay-Sachs disease. *J Biol Chem* 1987; **262**: 15396–15399.
- Borchelt DR, Thinakaran G, Eckman CB *et al*: Familial Alzheimer's disease-linked presenilin 1 variant elevates A $\beta$ 1-42/1-40 ratio *in vitro* and *in vivo*. *Neuron* 1996; **17**: 1005–1013.
- Mehta ND, Refolo LM, Eckman C *et al*: Increased A $\beta$ 42(43) from cell lines expressing presenilin 1 mutations. *Ann Neurol* 1998; **43**: 256–258.
- Citron M, Westaway D, Xia W *et al*: Mutant presenilins of Alzheimer's disease increase production of 42-residue amyloid beta-protein in both transfected cells and transgenic mice. *Nat Med* 1997; **3**: 67–72.
- Sandbrink R, Zhang D, Schaeffer S *et al*: Missense mutations of the *PS-1/S182* gene in German early-onset Alzheimer's disease patients. *Ann Neurol* 1996; **40**: 265–266.
- Ishii K, Ii K, Hasegawa T, Shoji S, Doi A, Mori H: Increased A $\beta$  42(43)-plaque deposition in early-onset familial Alzheimer's disease brains with the deletion of exon 9 and the missense point mutation (H163R) in the *PS-1* gene. *Neurosci Lett* 1997; **228**: 17–20.